



# Ab Initio Study of Stability, Local Order, and Phase Diagram For a Series of bcc-based Transition Metal Alloys

P. E. A. Turchi<sup>1</sup> · V. Drchal<sup>2</sup> · J. Kudrnovsky<sup>2</sup> · A. Perron<sup>1</sup>

Submitted: 18 May 2020 / in revised form: 13 August 2020 / Accepted: 4 September 2020 / Published online: 10 December 2020  
© ASM International 2020

**Abstract** A parameter-free electronic structure approach is applied to the study of stability and chemical order in the 15 substitutional body-centered cubic (bcc)-based alloys made of the six transition metals of groups 5 (V, Nb, Ta) and 6 (Cr, Mo, W) of the periodic table. The method is based on a Green's function description of the electronic structure of the random alloys. Configurational order is treated within the generalized perturbation method, and temperature effects are examined with a generalized mean-field approach. In contrast to the results summarized in the assessed phase diagrams, stability and ordering trends are predicted in a broad range of alloy composition for at least

seven alloys, and explanation is found in their electronic structure properties. Short-range order results, thermodynamics analysis, and bcc-based phase diagrams are also presented.

**Keywords** ab initio methods · metallic alloys · phase diagram · stability

## 1 Introduction

Much attention has been paid to alloys made of refractory transition metals (TM) of groups 5 (V, Nb, Ta) and 6 (Cr, Mo, W) of the periodic table (also referred to as columns VA and VIA in the old IUPAC labels), and in particular, Nb, Mo, Ta, and W that display high melting points. In this manuscript, the alloy notation is based on the group and period of the elements, i.e., V-Nb, V-Ta, V-Cr, V-Mo, V-W, Nb-Ta, Nb-Cr, Nb-Mo, Nb-W, Ta-Cr, Ta-Mo, Ta-W, Cr-Mo, Cr-W, and Mo-W. These alloys show excellent strength at elevated temperature and therefore have been found useful for high-temperature space and nuclear applications, among other applications. According to the fifteen reported phase diagrams,<sup>[1]</sup> most substitutional alloys should display complete solubility in the solid phase with a bcc (or  $\alpha$ ) crystalline structure before melting, except for the existence of a Laves phase (C14 and/or C15) in the case of V-Ta, Nb-Cr, and Ta-Cr, and a miscibility gap in the case of Cr-Mo and Cr-W. For the remaining ten bcc alloys of this class, no intermediate phases have been reported in the literature, although in some instances it has been claimed that chemical order “may” exist because of the variation of the lattice parameter with composition that shows a negative departure from Vegard's law,<sup>[2]</sup> and also

---

This article is an invited paper selected from presentations at “PSDK XIV: Phase Stability and Diffusion Kinetics—Gibbs: Phase Equilibria, Diffusion and Materials Design” held during MS&T'19, September 29–October 3, 2019, in Portland, Oregon. The special sessions were dedicated to honor Dr. Patrice Turchi, recipient of the ASM International 2019 J. Willard Gibbs Phase Equilibria Award “for outstanding and pioneering contributions in the application of first-principles, quantum-mechanical calculations to the modeling of phase equilibria and thermodynamic behavior of alloys.” It has been expanded from its original presentation.

---

✉ P. E. A. Turchi  
p.turchi@comcast.net

V. Drchal  
drchal@fzu.cz

J. Kudrnovsky  
kudrnov@fzu.cz

A. Perron  
perron1@llnl.gov

<sup>1</sup> Lawrence Livermore National Laboratory, Livermore, CA 94550

<sup>2</sup> Institute of Physics, Academy of Sciences of the Czech Republic, Na Slovance 2, 182 21 Praha 8, Czech Republic

of the activities of the alloy components determined at temperature that indicates negative deviation from Raoult's law, and therefore from ideality.<sup>[3]</sup> Furthermore, the measured negative excess free energies of mixing are attributed to mostly negative enthalpies of mixing and also small negative excess entropies of solution.<sup>[2,3]</sup> Let us review in more details what has been found so far experimentally.

In the case of **Cr-Mo**, a continuous series of solid solutions has been originally established,<sup>[4]</sup> but subsequent studies have revealed that it is a system that should exhibit a bcc miscibility gap.<sup>[1]</sup> For **Nb-Cr**, in addition to the existence of a bcc solid solution, a C15 Cr<sub>2</sub>Nb (of Cu<sub>2</sub>Mg-type) Laves phase has been identified.<sup>[4-6]</sup> Although the existence of a high-temperature C14 Cr<sub>2</sub>Nb (of MgZn<sub>2</sub>-type) Laves phase was initially reported, it was recently concluded that this phase was not thermodynamically stable, but only metastable and that diffraction lines from contaminations were mistaken for this phase.<sup>[5]</sup> For **Ta-Cr**,<sup>[7]</sup> both C14 Cr<sub>2</sub>Ta (high temperature) and C15 Cr<sub>2</sub>Ta (low temperature) phases have been reported. **V-Cr**<sup>[8]</sup> exhibits a continuous bcc solid solution in the solid-phase (however it is worth noting the “artistic” solidus–liquidus line in the reported phase diagram). **Cr-W** is a system that should exhibit a bcc miscibility gap.<sup>[1]</sup> Electromotive force (EMF) experiments<sup>[9]</sup> revealed that the enthalpy values for the **Nb-Mo** alloys are negative and relatively large, and since the excess integral entropies are small, the excess integral free energy are therefore almost equal to the integral enthalpies. Activities of Nb and Mo exhibit negative deviation from ideality, and the same is true from activities in the Ta-Mo system but negative deviation from ideality is smaller for the Nb-Mo system than for the Ta-Mo system. Small negative excess entropies could be attributed to the possible presence of short-range order

(SRO) in these alloys. And the highly negative heats of mixing indicate a preference for unlike pairs in these alloys. For **Ta-Mo**,<sup>[10]</sup> similar observations to those for Nb-Mo are applicable; SRO and size effect in a wide range of Ta-Mo alloy composition is primarily responsible for the cleavage fracture in the central part of the Ta-Mo phase diagram. Based on x-ray diffraction, B2 type order has been observed, although not explicitly specified by the authors, and once again, lattice parameter versus alloy composition shows a negative deviation from Vegard's law,<sup>[10]</sup> and the Gibbs energies versus composition measured at 1200 K exhibit high negative values.<sup>[11]</sup> **V-Mo**<sup>[12]</sup> and **Mo-W**<sup>[1]</sup> are considered as bcc solid solutions in the solid phase of the phase diagram. **V-Nb**, **Nb-Ta**, and **Nb-W** are considered as bcc solid solutions in the solid phase.<sup>[13]</sup> The phase diagram of **V-Ta** displays a bcc solid solution, and C15 V<sub>2</sub>Ta of Cu<sub>2</sub>Mg-type (at LT) and C14 V<sub>2</sub>Ta of MgZn<sub>2</sub>-type (at HT) Laves phases.<sup>[14-18]</sup> Based on EMF measurements, there is a negative deviation of the activities from ideality that is smaller in **Ta-W** than in Nb-Mo and Ta-Mo. The small negative values for the excess integral entropy of mixing has been attributed to vibrational contribution to the entropy and/or the presence of SRO.<sup>[3]</sup> Finally, **V-W** is still indicated as a case where bcc solid solution should exist in the solid part of the phase diagram.<sup>[1]</sup> This brief experimental review is summarized in Table 1.

These sparse experimental facts have led us to a reexamination of these fifteen alloy systems with a first-principles approach to stability and chemical order. Our focus will be primarily on the short-range order (SRO) taking place at high temperature and its extension to long-range order (LRO) at low temperature in the supposedly existing  $\alpha$  solid solution (note that phases that may develop with

**Table 1** Summary of experimentally known solid phases for the 15 binary phase diagrams made up of the six bcc transition metals

|    | Cr | Nb   | Mo                     | Ta   | W                       |
|----|----|--|------------------------|--|-------------------------|
| V  | SS | SS   | SS                     | LP (C15, C14)–V <sub>2</sub> Ta<br>LT and HT up to 1310 °C | SS                      |
| Cr |    | LP (C15)–Cr <sub>2</sub> Nb<br>up to 1770 °C | MG 880 °C<br>39 at% Mo | LP (C15,C14)–Cr <sub>2</sub> Ta<br>LT and HT up to 2020 °C | MG 1677 °C<br>50 at.% W |
| Nb |    |  | SRO                    | SS   | SS                      |
| Mo |    |  |                        | B2   | SS                      |
| Ta |    |  |                        |  | SRO                     |

SS = bcc solid solution, MG = bcc miscibility gap (maximum temperature and alloy composition), LP = Lave Phase(s) (in two cases a low (LT) and high (HT) temperature Laves phase, C15 and C14, respectively, have been reported) up to a temperature (in °C) associated with the LP-bcc SS transition. In red, the difference in the numbers of valence electrons,  $\Delta N = 0$ , and in blue,  $\Delta N = 1$  ( $N = 5$  for V, Nb, and Ta, and  $N = 6$  for Cr, Mo, and W). (For interpretation of the reference to color in this figure, the reader is referred to the web version of this article.)

structures other than bcc such as the tetragonal  $C11_b$  of  $MoSi_2$ -type will not be considered in this study). Needless to say that this chemical (or atomic, or spatial, or compositional) order plays a critical role in controlling materials properties, and as pointed out by Cahn<sup>[19]</sup> randomness in alloy structure is the exception rather than the rule, as it will be shown in this paper. To quote Cahn again, “The order–disorder transformation in alloys, and concerns associated with it, present a paradigm of modern physical metallurgy”.<sup>[19]</sup>

With the substantial literature that has been produced in recent years on high entropy alloys and its derivatives, this study becomes even more relevant. Indeed, since a couple of years ago, more and more studies have been published on the role of SRO and LRO in these alloys that were supposed to be single phase (either bcc, or fcc, or hcp-based solid solutions), but as emphasized before, solid solutions (i.e., chemically random alloys) are more the exception than the rule. Therefore, one should expect to generate chemical order or phase separation (that can be viewed as a special case of ordering) with a proper time-dependent heat treatment. For example in a recent paper,<sup>[20]</sup> the lattice parameter of the quinary W-Nb-Mo-Ta-V follows the rule of mixtures, hence is likely a case of fully disordered solid solution, whereas the quaternary W-Nb-Mo-Ta lattice parameter (obtained from composition average of the lattice parameters of the pure metals) is about 0.3% larger than the experimentally measured value, indicating that some solution ordering may be occurring, and this ordering can also be responsible for the absence of peaks from the crystallographic planes (222), (800), (660), etc., even though they are present in the x-ray diffraction pattern of the quinary alloy. As a reminder, it is worth noting that ordering in alloys was a very active and “fashionable” topic in the seventies and eighties, and indeed emphasized the impact of order on materials properties: i.e., not only thermal stability but also on electric, magnetic, and mechanical properties, fracture behavior, corrosion resistance, etc.

To discuss in a consistent way the results on stability and order as well as the trends for these fifteen bcc-based alloys, the configurational order will be examined within the generalized perturbation method (GPM).<sup>[21–22]</sup> The electronic structure properties of the reference medium on which the GPM relies will be described in the framework of the first-principles fully-relativistic self-consistent tight binding-linear muffin-tin orbital (TB-LMTO) multiple scattering formulation of the coherent potential approximation (CPA).<sup>[22–24]</sup> Finally, temperature effects on local order and stability will be examined by means of a standard generalized mean-field approach, namely the cluster variation method (CVM).<sup>[25]</sup>

The paper is organized as follows. In Sect. 2, we discuss the electronic structure methodology and properties of these alloys based on the first-principles TB-LMTO-CPA results. In Sect. 3, tendencies toward order or phase separation are examined in the context of the GPM. It will be shown that the nature and the strength of local order in these alloys can be well explained in terms of simple electronic parameters. In Sect. 4, the influence of temperature on stability and local order based on a standard generalized mean field approach will give us an opportunity to present the predicted coherent phase diagrams for this class of bcc-based alloys, before some concluding remarks summarized in Sect. 5.

## 2 Electronic Structure Methodology and Properties

Except in the case of the binary Ta-W<sup>[26]</sup> and the ternary Ta-Mo-W<sup>[27]</sup> systems, a systematic electronic structure-based study of these bcc alloys with a proper treatment of the disordered alloys has not been reported.

The motivation for the use of a quantum–mechanical based methodology is the need to perform an unbiased study on these alloys, in which the resulting thermodynamic behavior is determined on the basis of ab initio obtained interaction parameters that are free of imposed constraints, parametrization schemes, or fitting procedures. The mean-field single-site CPA,<sup>[22–23]</sup> expressed with the Green’s function formalism and implemented within the TB-LMTO-CPA,<sup>[24]</sup> provides an appropriate basis for such a study. This methodology allows us to define an effective medium whose scattering properties on the average reflect those of a chemically random alloy. Calculations based on this method yield relevant physical properties such as equilibrium lattice constants, energies of mixing, and bulk moduli for substitutionally disordered alloys. The effects of statistical local composition fluctuations away from this chemically disordered medium can be studied through the generalized perturbation method or GPM<sup>[21–22]</sup> that leads to uniquely defined, concentration-dependent effective cluster interactions (ECI). When used in conjunction with a statistical model, such as the cluster variation method (CVM),<sup>[25]</sup> these composition-dependent effective interactions and mixing energies lead to the prediction of the most stable ordered structures at zero temperature, and of concentration/temperature alloy phase diagrams.<sup>[28]</sup> For bcc-based chemically random alloys, electronic structure calculations were carried out on the basis of the charge self-consistent fully relativistic version of the TB-LMTO-CPA method<sup>[24]</sup> within the atomic sphere approximation (ASA) and the local density approximation (LDA) of density functional theory. The LDA calculations were based on the

exchange–correlation energy of Ceperley and Alder<sup>[29]</sup> as parameterized by Perdew and Zunger<sup>[30]</sup>. To eliminate the charge transfer effects, at each lattice parameter and alloy composition, the atomic sphere radii of the two species were adjusted in such a way that atoms were charge neutral while preserving the total volume of the alloy. Since the difference in the numbers of valence electrons is 0 or 1 for these fifteen alloys, very small charge transfer is expected, and therefore this approximation seems reasonable. In our calculations we used 168  $\mathbf{k}$ -points in the irreducible wedge of the Brillouin zone to perform the integrations that are necessary during the self-consistent calculations, and 2320  $\mathbf{k}$ -points in the full Brillouin zone for the calculation of the ECI. Twelve energy points on a semi-circle in the upper half-plane of complex energy were considered to perform the energy integration using Gauss' method. The densities of states were evaluated on a line 5 mRy above the real axis (with an energy step of about 5 mRy) and then deconvoluted on the real axis. The CPA equations were solved iteratively using the method described in Ref. 24.

By considering the number of valence electrons,  $N$ , and the difference in the numbers of valence electrons,  $\Delta N$ , we will consider in the following two categories of alloys:

(a) 6 alloys with  $\Delta N = 0$ , i.e., iso-electronic alloys from group 5 ( $N = 5$ : V-Nb, V-Ta, and Nb-Ta) and group 6 ( $N = 6$ : Cr-Mo, Cr-W, and Mo-W); and (b) 9 alloys with  $\Delta N = 1$  (for which  $N$  varies between 5 and 6 as a function of alloy composition: V-Cr, V-Mo, V-W, Nb-Cr, Nb-Mo, Nb-W, Ta-Cr, Ta-Mo, and Ta-W).

It is worth noting that although fully relativistic electronic structure calculations (i.e., by solving the Dirac equation) were carried out, spin polarization was ignored. The only systems that could have been affected by this approximation are those for which Cr is one component of the alloy. However Cr is the only element that displays a transition from anti-ferromagnetism (non-magnetic Cr) to a rather weak ferromagnetism (para-magnetic Cr) at 311 K, with the possibility of a more complex magnetic behavior—magnetism was not considered in this work.

In Fig. 1 the density of states of each of the six bcc-based transition metals (TM) are displayed. On the one hand, note that when  $N$  moves from 5 to 6, the Fermi energy spans a deep minimum of density of states that clearly separates the bonding and antibonding states, with high (low) densities of states (DOS) at the Fermi energy for  $N = 5$  (6); on the other hand, for each subgroup associated

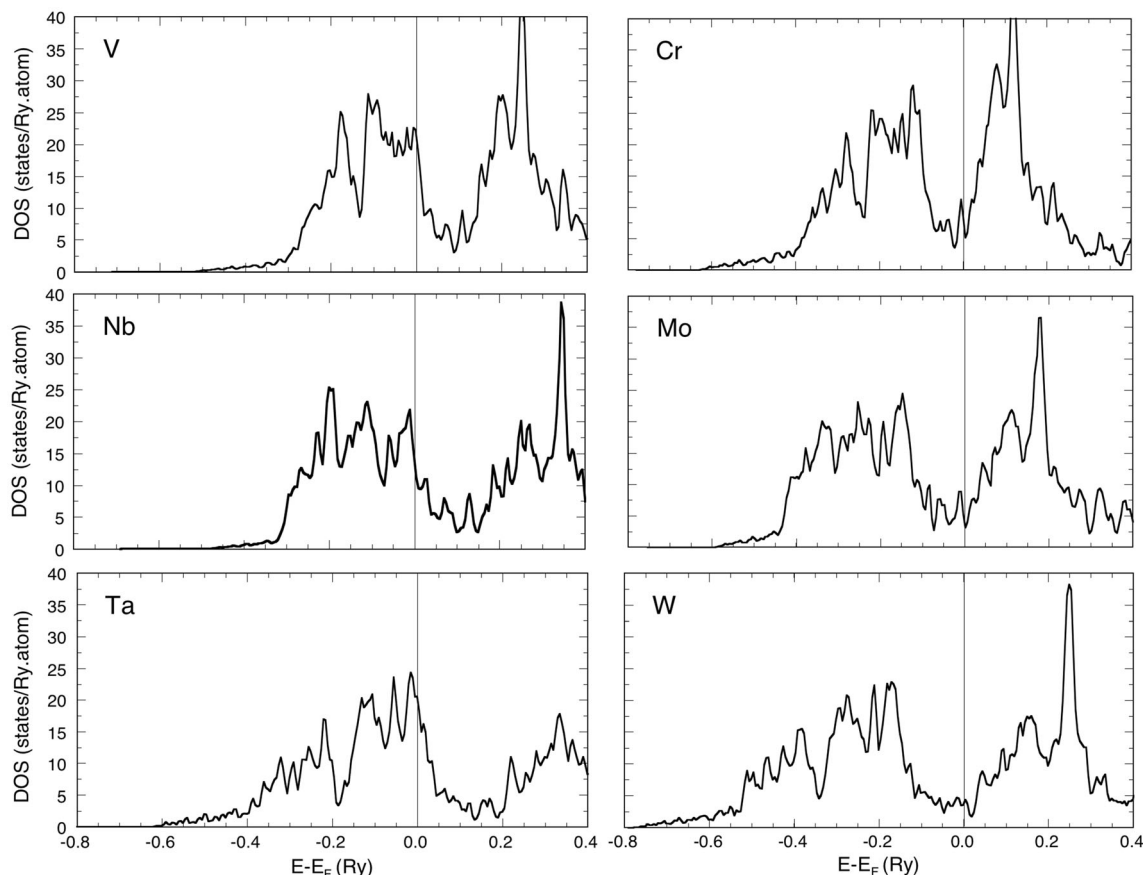


**Fig. 1** Electron density of states of the 6 bcc-based transition metals as a function of energy. The Fermi energy  $E_F$  (in Ry) is indicated by a vertical line and taken as zero of energy

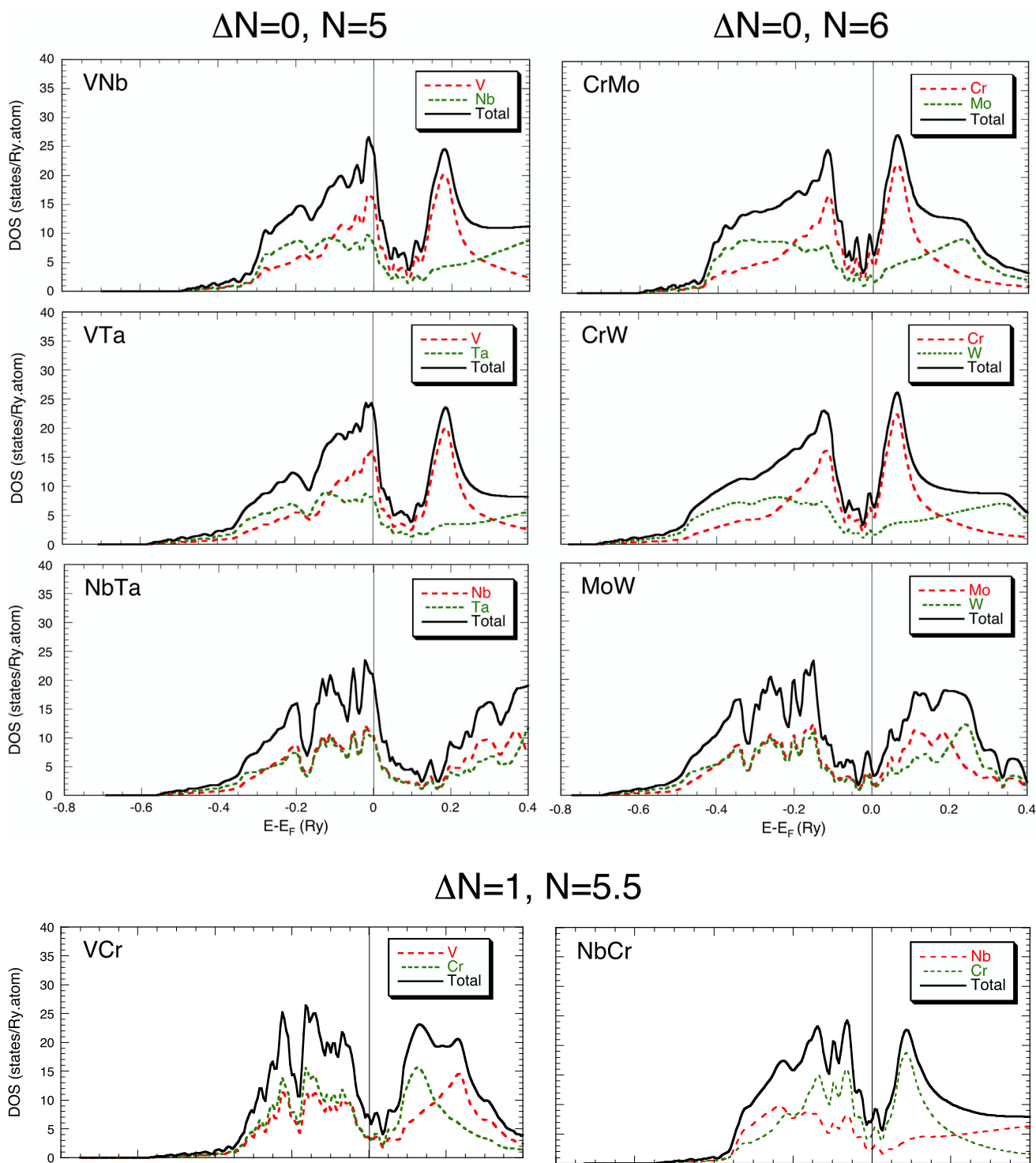


**Fig. 2** Electron density of states of the bcc-based chemically random alloys within the TB-LMTO-CPA at equi-atomic composition for  $\Delta N = 0$  and  $N = 5$  or  $6$  (top), and  $\Delta N = 1$  and  $N = 5.5$  (bottom) groups. The solid line indicates the total density of states, whereas the

dashed lines refer to the partial densities of states. The Fermi energy  $E_F$  (in Ry) is indicated by a vertical line and taken as zero of energy. (For interpretation of the references to color in this figure legend, the reader is referred to the web version of this article)

with  $N = 5$  and  $N = 6$ , the changes in the overall DOS, although mild, are due to an increase in the relativistic effects moving down from  $3d$  to  $4d$ , and  $5d$ .

In Fig. 2, the DOS of the chemically random alloys within the TB-LMTO-CPA at equi-atomic composition are displayed. For  $\Delta N = 0$  (and  $N = 5$  or  $6$ ), the DOS are rather

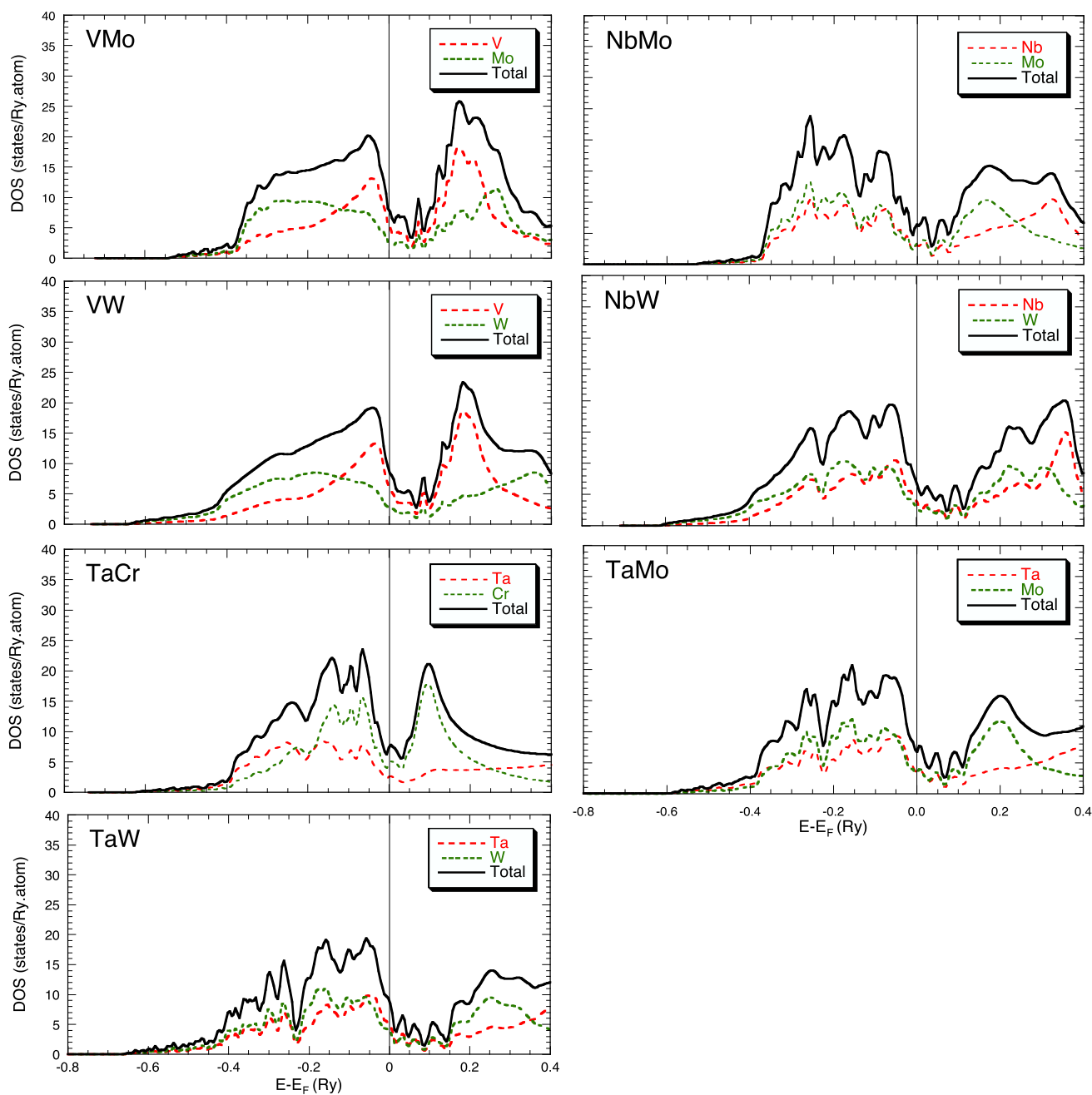


**Fig. 2** continued

similar to those of the pure metals, except for the disorder effect that translates in less structure in the features of the DOS, an effect that is even more pronounced in the case of chemically and topologically random alloys (i.e., amorphous alloys). In the case of the group of alloys with  $\Delta N = 1$ , the alloy species are neighbors in the periodic table, and therefore the scattering properties of the electrons, and the DOS remain practically unchanged with alloy composition (not shown). Since disorder is not major

for these alloys, the deep minimum observed in the DOS still corresponds to a clear separation between bonding and antibonding states in the alloy band structure, and the overall DOS, again, remain practically unchanged with alloy composition (not shown). The minimum in the DOS is, to some extent, related to a negative energy of formation, more so for the Cr, Mo, or W-rich alloys. Note also that the species-resolved DOS for the alloys are very similar to those associated with the pure metals. Thus the

variation of the electronic structure properties with alloy composition is almost entirely reflected in the variation of  $N$ , and therefore in the location of the Fermi energy, as would be the case for an alloy treated within the virtual-crystal approximation (VCA) or even the rigid-band model (RBM), despite the fact that chemical disorder is poorly treated within these two approximations (see below).

Some ab initio studies have been carried out by simulating alloy disorder within the so-called special quasi-random structure (SQS) approach.<sup>[31]</sup> This method assumes that one can generate a chemical “disorder” state by constructing a periodic ordered alloy structure with atomic pair correlation functions up to some distance that equate those of a truly disordered state of the same alloy. In other words, electronic structure properties of a SQS-based disordered alloy are those of an ordered structure, and this approach, although convenient for those who carry out ab initio calculations with wave-type method (such as VASP, WIEN2K, etc.), totally ignores the fundamental features of disorder such as the existence of a finite electron life time, one reason why DOS are never shown for disordered alloys built with this method. And one may wonder why this approach would systematically provide accurate results for derived quantities such as equilibrium properties, formation energies, elastic constant, and obviously transport properties for which the application of this method is highly arguable. Meanwhile this approach has been used in the past to study some of the alloys we are discussing in this paper such as Nb-Mo and Ta-W,<sup>[32]</sup> and Ta-W and V-W.<sup>[33]</sup>

Another method that has been used to deal with disorder is the VCA [see Ref. 34 for details]. As in the case of the SQS method, VCA cannot handle truly chemical random states, since this method is also dealing with a periodic lattice and the design of a virtual “average” atom on each site that interpolates between the behavior of the actual alloy components, hence preserving the periodicity of the lattice. Once again, the pitfalls of the SQS apply to this method, which is, in addition, mathematically flawed.<sup>[34]</sup> For completeness, the simplest and most basic approximation is based on the RBM, which consists in taking a composition average of the DOS of the pure alloy constituents and fixing the Fermi energy to the one that corresponds to the proper average number of electrons per atom. Once again, this method is not well suited to account for chemical disorder in alloys.

In Fig. 3 (top) the lattice parameter at 0 K of each bcc TM is shown, and the 3d electrons-type metals (V, Cr) are clearly distinguished from the 4d (Nb, Mo) and 5d (Ta, W) ones. There is about a 1% discrepancy as generally observed between the ab initio and experimental values.

In Fig. 3 (bottom), the bulk modulus at 0 K for each TM is shown, and there is a typical 15% discrepancy between predicted and measured values. In this case, the distinction

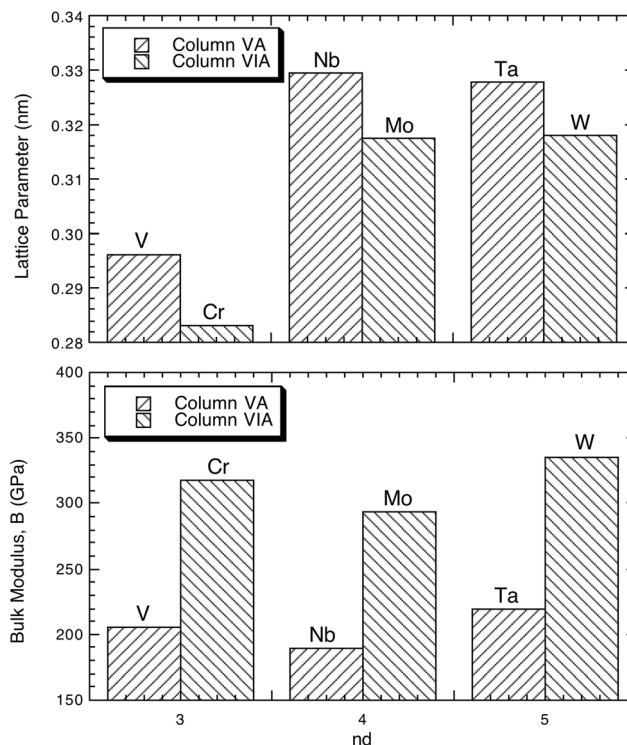


**Fig. 3** Lattice parameter (top), in Å, and bulk modulus (bottom), in GPa, at  $T = 0$  K, are shown for 3d, 4d, and 5d electrons-type bcc transition metals

between metals from groups 5 (V, Nb, Ta) and 6 (Cr, Mo, W) is worth noting. One should also note that, as observed experimentally, a one-valence electron difference leads to a 50% or more increase in the bulk modulus. The variation of the lattice parameter and bulk modulus with alloy composition is shown for all 15 bcc-based TM alloys in Fig. 4, and the departure of the lattice constant from Vegard’s law, although small, is an indication that a tendency towards alloy formation and order is expected.

Finally, in Fig. 5 the variations of the mixing (or formation) energy of the chemically random alloy versus composition are shown. This energy is given by

$$\Delta E_{\text{Mix}} = E_{\text{Alloy}}^{\text{CPA}} - c_A E_A^{\text{Eq}} - (1 - c_B) E_B^{\text{Eq}} \quad (\text{Eq 1})$$

where  $E_{\text{Alloy}}^{\text{CPA}}$  is the total energy of the alloy described within the CPA at its equilibrium lattice parameter, and  $E_i^{\text{Eq}}$  is the total energy of pure species  $i$  at its corresponding equilibrium lattice parameter. As a reminder, a negative (positive) mixing energy favors the formation (phase separation) of the random alloy.

As shown in Fig. 5, the mixing energies in the whole range of alloy composition are negative for  $\Delta N = 0$  except for Mo-W which exhibits insignificantly positive mixing energy. Small negative magnitude is also observed in the case of Nb-Ta, V-Nb, and Cr-Mo ( $\Delta N = 0$ ). As for  $\Delta N = 1$ , slightly positive values are found for Nb-Cr.

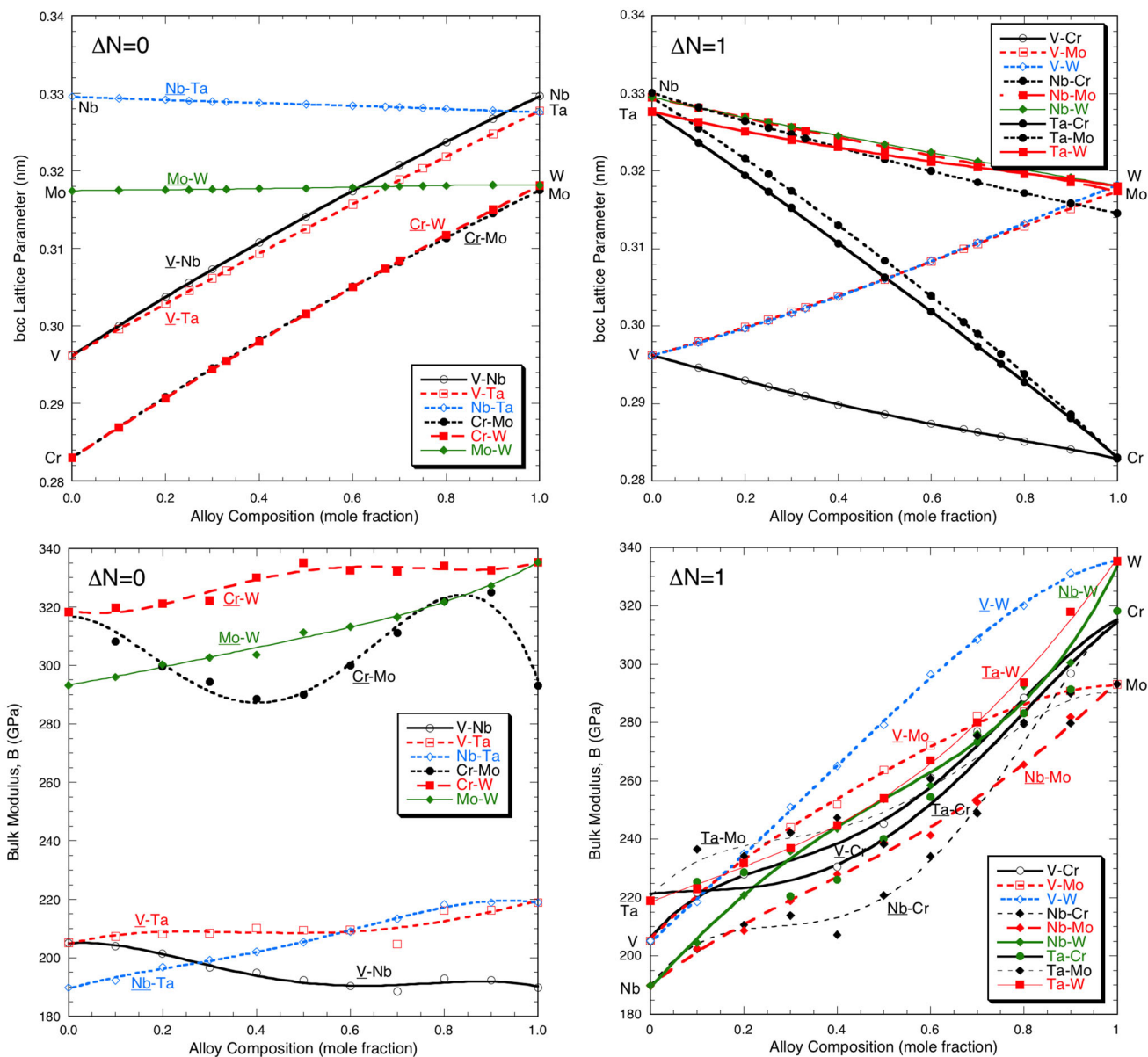


**Fig. 4** Variation of the lattice parameter (top), in Å, and bulk modulus (bottom), in GPa, with alloy composition for all 15 bcc-based TM alloys. For all alloys the composition along the horizontal

axis refers to the second element of each alloy. (For interpretation of the references to color in this figure legend, the reader is referred to the web version of this article)

These results confirm a previous conclusion drawn from a semi-empirical tight-binding (TB) estimation of the energy of formation of the random Ta-W alloy as a function of composition.<sup>[35]</sup> However in this earlier study, the tight-binding energies were underestimated by about 40%, and the general evolution of the formation energy with alloy composition did not reveal any asymmetry as it should since the DOS at the Fermi energy that controls the strength of the bonding in this alloy varies significantly with the number of valence electrons. The same TB approach has been applied to bcc-based Cr-Mo, Cr-W, and Mo-W alloys, with similar output.<sup>[36]</sup> Based on the use of

the VASP code<sup>[37–39]</sup> for the description of the electronic structure and the SQS approach to deal with “chemical disorder”, mixing enthalpies have been calculated for V-Nb, and Nb-Ta ( $\Delta N = 0$ ), V-Mo, Nb-Mo, and Ta-Mo ( $\Delta N = 1$ ).<sup>[40]</sup> With a similar approach, “random” alloy enthalpies have been reported for Nb-Mo, Nb-W, Ta-Mo, and Ta-W in Ref. 41. Both studies<sup>[40,41]</sup> provide results that are qualitatively in agreement with those presented in the present work.



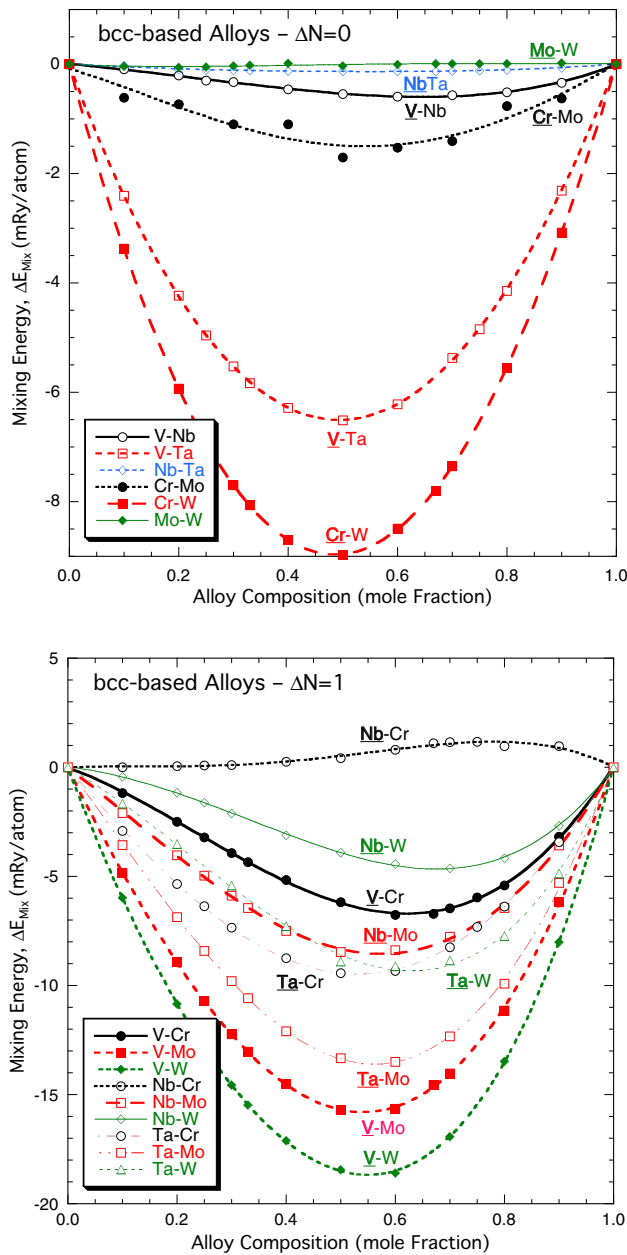


**Fig. 5** Variation of the mixing energy  $\Delta E_{\text{Mix}}$  (in mRy/atom) of the bcc-based chemically random alloys with composition, within the TB-LMTO-CPA for (top)  $\Delta N = 0$  and (bottom)  $\Delta N = 1$  groups. For all alloys the composition along the horizontal axis refers to the second element of each alloy. (For interpretation of the references to color in this figure legend, the reader is referred to the web version of this article)

### 3 Ground-State Properties

In recent years, a number of methods have been developed<sup>[28]</sup> to map the quantum mechanical description of the energetics of an alloy in the form of an Ising model, which is most appropriate for a subsequent statistical-mechanics treatment of order–disorder phenomena in alloys as

functions of temperature and composition. This mapping has been originally achieved within the so-called generalized perturbation method (GPM),<sup>[21,22]</sup> which will be used here. Within the GPM, “only the configuration-dependent contribution to the total energy is expressed by an expansion” in terms of effective pair and multi-site interactions, and since the reference medium, which, in the case of the GPM, is the chemically random state of the alloy, the terms that populate the expansion are composition-dependent, so are these interactions. One should emphasize that this method is in contrast with the ones based on the knowledge of the electronic structure properties of ordered configurations of the alloy, such as the so-called Connolly–Williams Method (CWM),<sup>[42]</sup> which lead to “an expansion of the total energy itself in terms of cluster interactions” which are composition-independent, except via volume effects. Within the GPM, the ordering contribution to the total energy of an A–B alloy is given by

$$\delta E_{\text{Ord}}(\{p_n\}) = \sum_{k=1}^{\infty} \frac{1}{k} \sum_{n_1 \dots n_k} V_{n_1 \dots n_k}^{(k)} \delta c_{n_1} \dots \delta c_{n_k} \quad (\text{Eq 2})$$

where  $\delta c_{n_i}$  refers to composition fluctuation on site  $n_i$ ,  $\delta c_{n_i} = p_{n_i} - c$ , around the average composition of the random medium, characterized by  $c$  that is the composition in B-species, and  $p_{n_i}$  is an occupation number associated with site  $n_i$ , equal to 1 or 0 depending on whether or not site  $n_i$  is occupied by a B-species.  $V_{n_1 \dots n_k}^{(k)}$  corresponds to a  $k$ th-order ECI involving a cluster of  $k$  sites. The prime in the summation over the  $n_i$  indicates that consecutive site indices must be different. Note that, as in any perturbation theory that relies on the CPA medium, the small parameter in the GPM only depends on the scattering properties of the electrons (and not the composition), which means that the expansion for the ordering energy is valid even for large fluctuations of local composition. In practice, the second order contribution to the ECI,  $V_{nm}^{(2)}$  is, within the GPM, essentially numerically indistinguishable from the full summation of all scattering processes taking place between the two sites  $n$  and  $m$ . Hence, to second order in perturbation (i.e.,  $k \leq 2$ ), and for alloys based on simple lattices described by one type of site per cell, such as bcc, Eq. 2 is rewritten as

$$\Delta E_{\text{Ord}}(\{p_n\}) \approx \sum_s V_{0s}^{(2)} \delta c_0 \delta c_s \quad (\text{Eq 3})$$

or equivalently, at zero temperature

$$\Delta E_{\text{Ord}}(\{q_s\}) \approx \sum_s q_s V_s \quad (\text{Eq 4})$$

with  $q_s = \frac{c}{2} (n_s^{\text{BB}} - cn_s)$ , where  $n_s^{\text{BB}}$  and  $n_s$  refer to the number of BB pairs and the total number of pairs per site,

respectively, associated with the  $s$ th-neighbor shell, and  $c$  is the composition in  $B$  species.

In this last equation, the effective pair interaction (EPI)  $V_s$  represents a  $s$ th EPI given by  $V_s = V_s^{AA} + V_s^{BB} - 2V_s^{AB}$  that, by definition, corresponds to the 2<sup>nd</sup>-order interaction  $V_{0s}^{(2)}$ , entering Eq. 3, between a site at the origin and a site belonging to the  $s$ th-neighbor shell. In the following the superscript “(2)” of  $V$  will be dropped out:  $V_s \equiv V_{0s}^{(2)}$ . Hence, the sign convention that has been adopted is such that when  $V_s > 0$  ( $< 0$ ), AB (AA or BB) pairs associated with a species at the origin and the other in the  $s$ th-neighbor shell are favored. As seen from Eq. 4, any alloy configuration is specified by a unique set of parameters  $q_s$  that only depends on site occupancies. For example, at zero temperature and for  $s = 1-5$ , these parameters take the values  $(-1, 3/4, 3/2, -3, 1)$  for B2 order (of CsCl-type;  $cP2$ ;  $Fm\bar{3}m$ ) and  $(0, -3/4, 3/2, 0, -1)$  for B32 order (of NaTl-type;  $cF16$ ;  $Fd\bar{3}m$ ) at equi-atomic composition, and  $(-1/4, -3/16, 9/8, -3/4, -1/4)$ , for  $DO_3$  order (of  $Fe_3Al$ -type;  $cF16$ ;  $Fm\bar{3}m$ ) at  $c = 1/4, 3/4$ .

In this context, phase separation (segregation or clustering) can be considered as a particular state of order for which  $q_s = c(1-c)n_s/2$  (since  $n_s^{BB} = n_s$ ) with, for a bcc lattice,  $n_s = 8, 6, 12, 24, 8$  ( $s = 1-5$ ). As explained in Ref. 43, the clustering energy is estimated from the concentration-weighted average of the DOSs of the pure metals, each calculated at the average Fermi level of the average CPA medium, in the spirit of the GPM. On the other hand, the formation energy of the alloy is obtained from the contribution of the two sub-bands that are associated with each species and its own Fermi level. As long as the interfacial energies are negligible (which would be the case for alloy species exhibiting similar electron scattering properties; an assumption that is applicable to the present class of alloys), it is expected that the total energies that correspond to both situations (i.e., segregation within an alloy sample and juxtaposition of two metals) to be the same. Hence, in the following, the formation energy of the alloy will be approximately given by  $-\Delta E_{Seg}$ .

It is worth noting that B2 and B32 can be described as layered structures with one (two) layer(s) of A species and one (two) layer(s) of B species along the [111] direction of the bcc lattice, as compared to the segregated state where the bcc lattice is fully occupied by A (or B) species only.

Before presenting the results, it is worth commenting on the major differences between the GPM and the CWM,<sup>[42]</sup> or as it is referred now by the cluster expansion method (CEM). In the case of the GPM, the formation energy of a particular alloy configuration  $\phi$  is given by:

$$\Delta E_{Alloy}^{\phi} = \Delta E_{Mix} + \Delta E_{Ord}^{\phi} \quad (\text{Eq 5})$$

where  $\Delta E_{Mix}$  and  $\Delta E_{Ord}^{\phi}$  are the mixing energy of the disordered alloy and the ordering energy given by Eqs. 1 and 3 (or 4), respectively. And both energies depend on alloy composition. Note that the ordering depends directly on composition through the  $\{q_s\}$  in Eq. 4, but also through the composition-dependence of the interactions themselves that are formulated with reference to the disordered medium, also composition dependent. This formulation allows an alloy to be stable in the chemically random state and displays at the same time a tendency towards phase separation (because of the decoupling between the mixing energy of the disordered state and the ordering energy). Similarly, an alloy can display ordering in some composition range and phase separation in another range (because of the composition dependence of both the mixing energy of the disordered state and the ordering energy). Finally, the method that has been discussed here is valid for binary alloys but can be easily extended to multi-component alloy systems. Now a question that has been raised in many occasions on this GPM approach concerns the role of multi-component interactions beyond the pair interactions. This question relates to the more fundamental definition and significance of an interaction in an alloy. According to the GPM, the scattering of electrons is what governs the sign and magnitude of an EPI according to the following equation:

$$V_{pq} = -\frac{\Im m}{n\pi} \int_{-\infty}^{E_F} d\varepsilon (\Delta t)^2 \sum_{\lambda\mu} \left( \langle G_{pq}^{\lambda\mu} \rangle \right)^2 \quad (\text{Eq 6})$$

where  $n$  is the number of orbital (9 orbitals in the present case since  $s, p$  and  $d$  electrons are included in the ab initio calculations),  $\Delta t = t^A - t^B$ , with  $t^i$  being an onsite energy associated with species  $i$  (A or B), and  $\langle G \rangle$  is an off-diagonal in site component of the Green function for a particular set of orbitals  $\lambda$  and  $\mu$  and sites  $p$  and  $q$ , and the integral is considered up to the Fermi energy. The  $G$ 's decrease rapidly with distance, and for an ECI that involves a cluster of more than two sites, this Eq. 6 can be easily generalized, and now, instead of a product of two  $G$ 's, this product involves a number of  $G$ 's corresponding to the number of sites considered to describe the ECI. It is this product that rapidly decreases with the number of sites, and based on our experience with the application of the GPM to many transition metals alloys, usually the expansion in Eq. 2 is converged by considering the nearest EPIs and excluding any ECI. In conclusion, this method provides a way to predict ordering in alloys by considering the response of a reference medium (here the chemically random state of the alloy as described by the CPA) to

composition fluctuations and its energetics. It becomes clear that the strength of an interaction between two sites should be affected by the surrounding composition, and more generally to the surrounding topology as it would be the case for amorphous alloys. This property required physical metallurgists to recognize its importance, and the first experimental report on SRO effects in Fe-Cr alloys<sup>[44]</sup> confirmed the relation between ordering and electronic properties of the EPIs.

Now in the case of the CEM, the formation energy of a given alloy configuration is given by the following equation:

$$\Delta E_{\text{Form}}^\phi = V_0 + \sum_{\alpha} \left( \sigma_1^\phi \sigma_2^\phi \cdots \sigma_{\alpha}^\phi \right) V_{\alpha} \tag{Eq 7}$$

where

$$\Delta E_{\text{Form}}^\phi = E^\phi - \left( 1 - c_B^\phi \right) E_A - c_B^\phi E_B \tag{Eq 8}$$

with  $\sigma_n^\phi = 2p_n^\phi - 1$  is equal to  $-1$  or  $+1$  depending of the occupation of a site  $n$  by an A or a B species, and  $V_{\alpha}$  is an interaction associated with a cluster of  $\alpha$  sites. Note that in this case the mixing energy of the disordered state configuration “Dis” is specified by the same interactions that describe a specific alloy configuration  $\phi$  according to:

$$\Delta E_{\text{Form}}^{\text{Dis}} = V_0 + \sum_{\alpha} (2c - 1)^{\alpha} V_{\alpha} \tag{Eq 9}$$

In practice, the formation energy associated with each  $\phi$  of a large set of configurations and the knowledge of the  $\{\sigma_{\alpha}^\phi\}$  for each sub-cluster  $\alpha$  included in a maximum cluster allows to solve the system of equations that will return the interactions  $\{V_{\alpha}\}$ . The CEM is easy to implement and is not limited to any structure (as practically the case for the GPM approach). However, there is the question about the number and type of clusters, and the selection of the ordered configurations  $\{\phi\}$  that need to be selected. Note also that the interactions are composition independent (except via volume effect), and it was shown in practice that the expansion defined in Eq. 7 slowly converges in terms of interactions. Besides these aspects of the CEM, more fundamental questions have been raised,<sup>[45]</sup> and despite technical progress on this methodology,<sup>[46-47]</sup> additional questions have been raised by one of the originators himself of the methodology.<sup>[48-49]</sup> The only viable version of the CEM would be to account like in the GPM on the composition dependence of the interactions, and this could be implemented easily by generating at each alloy composition  $c$  a set of configurations,  $\phi_i(c)$ , and solving for the pair and multi-site interactions: this would corresponds to developing a CEM in the canonical ensemble. The only remaining major difference with the GPM approach would be about the assumption that the chemically random state

of the alloy should be defined with the same interactions as those that describe any ordered state at a given composition, an assumption that has been rejected in the past.

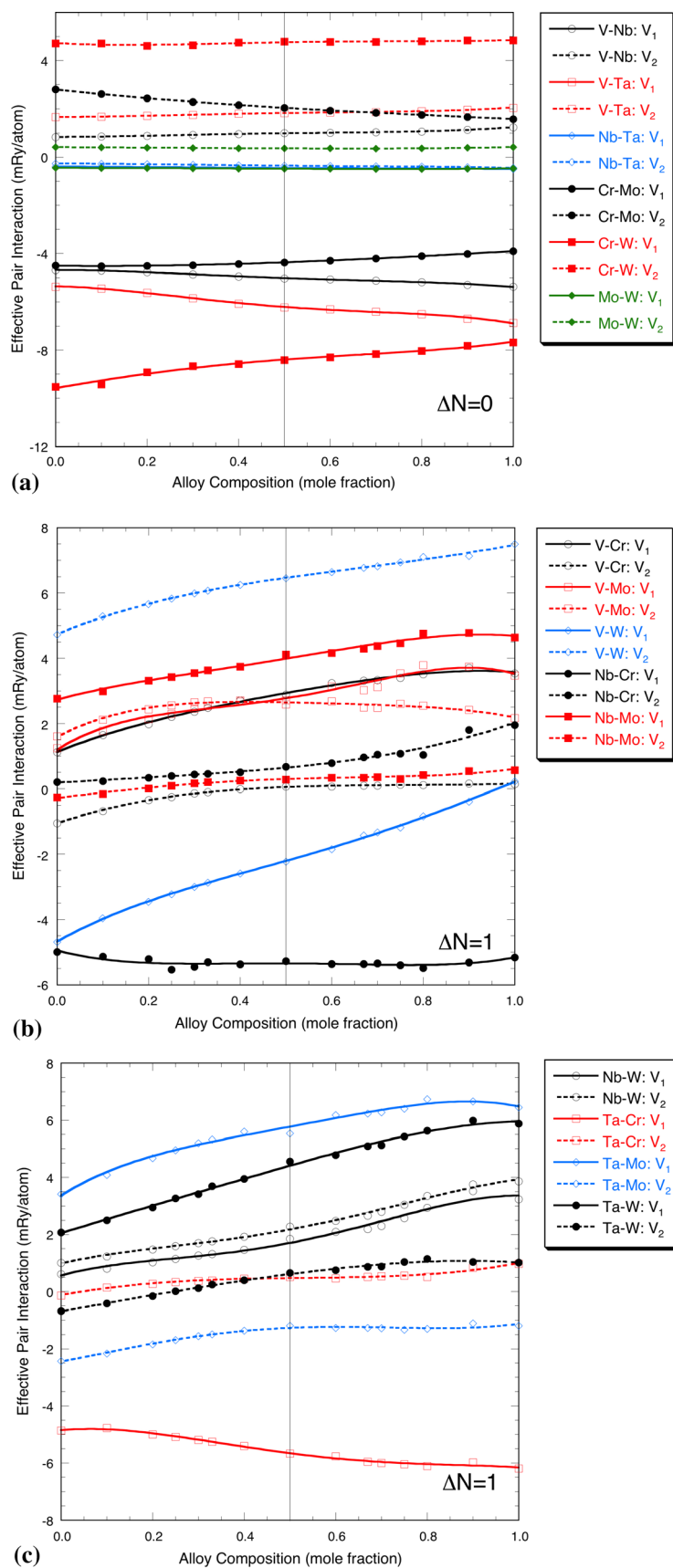
The first and second nearest neighbor EPIs,  $V_1$  and  $V_2$ , are shown as functions of composition for the 15 bcc-based TM alloy as obtained from TB-LMTO-CPA-GPM in Fig. 6. The EPIs beyond the 2nd nearest neighbors are at least an order of magnitude smaller than the first two EPIs, as shown in Fig. 7 for five alloys at equi-atomic composition as examples; and the same applies to multi-site effective interactions (not shown). Also, we found that each EPI varies very little with the lattice parameter (not shown), and therefore with pressure, at any alloy composition. There is also a variation in the magnitude of the EPIs with alloy composition, but rarely a change in sign is observed. Overall, the ordering tendencies are stronger for the A–B alloys with B belonging to Group 6 of the periodic table, and this trend is consistent with what is expected for transition metal alloys.<sup>[22-28]</sup> Indeed, the variation of the dominant EPIs displays as a function of the number of  $d$ -electrons two zeros which are located around  $3d$  and  $7d$ -electrons, with a positive sign of the EPIs in the central region. Although the location of the zeros varies with the scattering properties of the electrons and alloy composition, hetero-atomic pairs are increasingly favored when the number of  $d$ -electrons increases from A (about  $3d-\bar{e}$ ) to B (about  $4d-\bar{e}$ ), which is what Fig. 6 shows in a more quantitative way.

According to the results of the ground-state analysis of the Ising Hamiltonian applied to the bcc lattice<sup>[22]</sup> with first and second nearest pair interactions, B2, B32, and  $DO_3$  are the most probable ground states at zero temperature (see Fig. 8), in addition to phase separation (N.B.: the analysis of the Ising model has been extended up to the fifth neighbor pair interaction, with the exclusion of  $V_4$ , in Refs. 50-52). The resulting ordering map in the  $\{V_1, V_2\}$  space is displayed for all fifteen bcc-based TM alloys at equi-atomic composition in Fig. 9; and a summary of the results are given in Table 2 with its quantitative counterpart in Table 3. As a reminder, by accounting for composition-dependent EPIs, the trajectory around each point associated with an alloy in Fig. 9 is very limited according to Fig. 6, and therefore does not modify the ground-state predictions that were made exclusively at equi-atomic alloy composition. Finally, it is worth noting that a B32 ordered state is predicted for V-Mo, V-W, and Nb-W, which is rather unusual for TM alloys since it is found in compounds such as NaTi.

### 4 Stability at Finite Temperature

To extend the study at finite temperature, the Ising model has been solved within a generalized mean-field approximation with the CVM<sup>[25]</sup> in the canonical ensemble (i.e., at

**Fig. 6** First and second nearest neighbor effective pair interactions,  $V_1$  and  $V_2$ , in mRy/atom, as functions of composition for bcc-based alloys, as obtained from TB-LMTO-CPA-GPM. Top figure for alloys characterized by  $\Delta N = 0$  and the bottom two for  $\Delta N = 1$ . For all alloys the composition along the horizontal axis refers to the second element of each alloy. (For interpretation of the references to color in this figure legend, the reader is referred to the web version of this article)



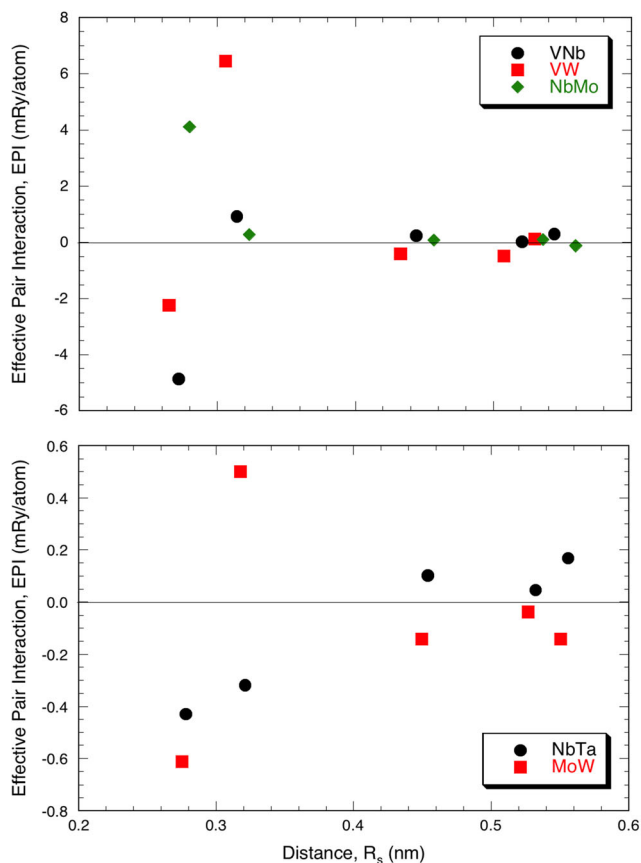


**Fig. 7** Effective pair interactions, in mRy/atom, as functions of distance, as obtained from TB-LMTO-CPA-GPM, for bcc-based VNb, VW, and NbMo (top), and NbTa and MoW (bottom). (For interpretation of the references to color in this figure legend, the reader is referred to the web version of this article)

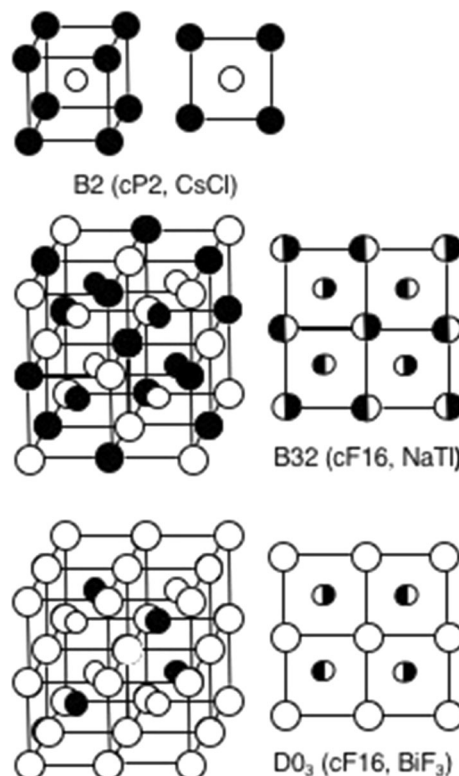


**Fig. 8** Description of the B2, B32 and  $D0_3$  ordered structures based on the bcc lattice

constant alloy composition) by making use of the energetics (i.e., mixing energies and EPIs) presented in Sect. 2 and 3. At each temperature and alloy composition, the configurational part of the free energy has been minimized with a Newton–Raphson technique with respect to the

**Fig. 9** Ground state analysis of the Ising model applied to the fifteen bcc-based transition metal alloys. The first and second effective pair interactions (in mRy/atom) for each alloy at equi-atomic composition are plotted in the  $\{V_1, V_2\}$  ordering map, in a domain where the most stable ground state is indicated. “A” in this map refers to phase separation whereas B2, B32 and  $D0_3$  are described in Fig. 8. (For interpretation of the references to color in this figure legend, the reader is referred to the web version of this article)

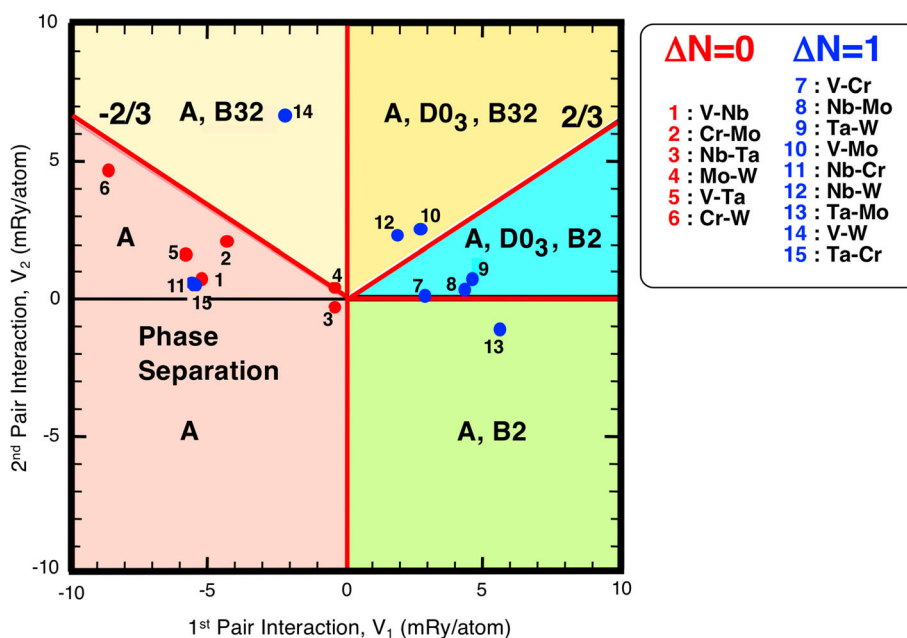


**Table 2** Summary of the ab initio theoretical predictions of the bcc ordering tendency (no other phases such as the existence of Laves phase is considered) at equi-atomic composition for the fifteen binary alloys made up of the six bcc transition metals

|    | Cr | Nb | Mo  | Ta | W   |
|----|----|----|-----|----|-----|
| V  | B2 | MG | B32 | MG | B32 |
| Cr |    | MG | MG  | MG | MG  |
| Nb |    |    | B2  | MG | B32 |
| Mo |    |    |     | B2 | B32 |
| Ta |    |    |     |    | B2  |

The color code is the same as for Table 1. (For interpretation of the reference to color in this table, the reader is referred to the web version of this article.)

**Table 3** All energies are given in mRy/atom at equi-atomic composition

| Alloy          | $\Delta E_{\text{Mix}}$ | EPI $V_1$ | EPI $V_2$ | $\Delta E_{\text{B2}}$ | $\Delta E_{\text{B32}}$ | $\Delta E_{\text{Seg}}$ |
|----------------|-------------------------|-----------|-----------|------------------------|-------------------------|-------------------------|
| $\Delta N = 0$ |                         |           |           |                        |                         |                         |
| CrW            | - 8.971                 | - 8.663   | + 4.637   | + 12.14                | - 3.48                  | - <b>5.19</b>           |
| VTa            | - 6.510                 | - 5.855   | + 1.754   | + 7.17                 | - 1.31                  | - <b>4.54</b>           |
| VNb            | - 0.548                 | - 4.860   | + 0.910   | + 5.55                 | - 0.69                  | - <b>4.17</b>           |
| CrMo           | - 1.709                 | - 4.364   | + 2.047   | + 5.90                 | - 2.02                  | - <b>2.83</b>           |
| NbTa           | - 0.133                 | - 0.429   | - 0.318   | + 0.19                 | + 0.24                  | - <b>0.67</b>           |
| MoW            | - 0.035                 | - 0.467   | + 0.381   | + 0.75                 | - <b>0.29</b>           | - 0.18                  |
| $\Delta N = 1$ |                         |           |           |                        |                         |                         |
| VCr            | - 6.179                 | + 2.886   | + 0.066   | - <b>2.84</b>          | - 0.05                  | + 2.95                  |
| NbMo           | - 8.464                 | + 4.119   | + 0.279   | - <b>3.91</b>          | - 0.21                  | + 4.33                  |
| TaW            | - 8.893                 | + 4.561   | + 0.658   | - <b>4.07</b>          | - 0.49                  | + 5.05                  |
| VMo            | - 15.699                | + 2.719   | + 2.588   | - 0.78                 | - <b>1.94</b>           | + 4.66                  |
| NbCr           | + 0.429                 | - 5.285   | + 0.670   | + 5.79                 | - 0.50                  | - <b>4.78</b>           |
| NbW            | - 3.910                 | + 1.846   | + 2.278   | - 0.14                 | - <b>1.71</b>           | + 3.55                  |
| TaMo           | - 13.328                | + 5.543   | - 1.188   | - <b>6.93</b>          | + 0.89                  | + 4.65                  |
| VW             | - 18.442                | - 2.227   | + 6.447   | + 7.06                 | - <b>4.84</b>           | + 2.61                  |
| TaCr           | - 9.431                 | - 5.672   | + 0.516   | + 6.06                 | - 0.39                  | - <b>5.29</b>           |

$\Delta E_{\text{Mix}}$  is the mixing energy, the next two columns indicate the magnitude of the first and second nearest neighbor EPIs,  $\Delta E_{\text{B2}}$  and  $\Delta E_{\text{B32}}$  are the ordering energies associated with the B2 and B32 ordered states, and  $\Delta E_{\text{Seg}}$  is the energy associated with the segregated state, all based on the bcc lattice. For each alloy the number identified in bold corresponds to the energy at equi-atomic composition of the most likely stable ordered state

correlation functions defined as the following thermodynamic average product:

$$\xi_\alpha = \langle \sigma_1 \cdots \sigma_\alpha \rangle \quad (\text{Eq 10})$$

where  $\sigma_n$  corresponds to the so-called spin variable defined in Eq. 7, and the maximum value of  $\alpha$  corresponds to the

number of sites in the maximum cluster that characterizes the level of approximation of the CVM. In the present case, the maximum cluster corresponds to the irregular tetrahedron made of four first and two second-nearest-neighbor pairs.<sup>[53-54]</sup> This cluster allows a proper statistical treatment with the EPIs  $V_1$  and  $V_2$  included in the pair expansion of the Ising model, an approximation which is justified here since the more distant EPIs have negligible amplitude, see Fig. 7. Hence the ab initio information for  $\Delta E_{\text{Mix}}$  (see Eq. 1 and Fig. 5) and the EPIs (see Eq. 6 and Fig. 6),  $V_1$  and  $V_2$ , are used to carry out the CVM calculations of the Gibbs energy as a function of alloy composition and temperature for each of the fifteen alloy systems.

The predicted phase diagrams shown in Fig. 10 that are likely to need to be confirmed are: V-Cr, Nb-Mo, Ta-Mo, Ta-W that display a domain of stability of the ordered B2 phase, and V-Mo, V-W, and Nb-W that exhibit a region of B32 order. In the case of V-Cr and Ta-W a domain of stability of the  $\text{D0}_3$  ordered phase around  $\text{VCr}_3$  and  $\text{TaW}_3$ , respectively, has not been reported in the phase diagrams since the order-disorder transitions are below 75 and 200 K, respectively. Confirmation of a miscibility gap is also required in the newly predicted V-Nb, V-Ta, Nb-Cr, and Ta-Cr alloy systems (above 1000 K), in addition to Cr-Mo and Cr-W that have been already confirmed experimentally.<sup>1</sup> Two phase diagrams have not been discussed: those of Nb-Ta and Mo-W, since for both systems, extremely small magnitudes of the mixing energy and the EPIs that build up the ordering contribution to the formation energy lead practically to an ideal behavior, i.e., the existence of a bcc-based solid solution, which is indeed more the exception than the rule. The asymmetry of some phase diagrams is a direct consequence of the alloy energetics, i.e., an extremum of energy of mixing, and stronger ordering trends in some composition range away from equi-atomic composition. For this class of phase separating alloys ( $\Delta N = 0$ ), Fig. 11 shows that along groups 5 ( $N = 5$ ) and 6 ( $N = 6$ ), the trends are very similar for both the mixing energy and the first and second neighbor EPIs with higher magnitudes for the  $3d-5d$  mixtures than for the  $3d-4d$  ones, and this is reflected in the location of the top of the miscibility gap for the respective alloys. In the case of the other subset of alloys ( $\Delta N = 1$ ), there is a trend associated to which row the elements belong to ( $3d$ ,  $4d$ , or  $5d$ ), whereas for the remaining mixtures, a more subtle evolution exists. The same remark applies to the evolution of the first and second EPIs.

Despite the noticeable difference in the elastic properties of group 5 and 6 elements (see Fig. 3), one could question the absence of vibrational contribution to the Gibbs energy in the present treatment. Based on calculations carried out for Ta-W alloys,<sup>[26]</sup> it has been found that the vibrational free energy is more than an order of

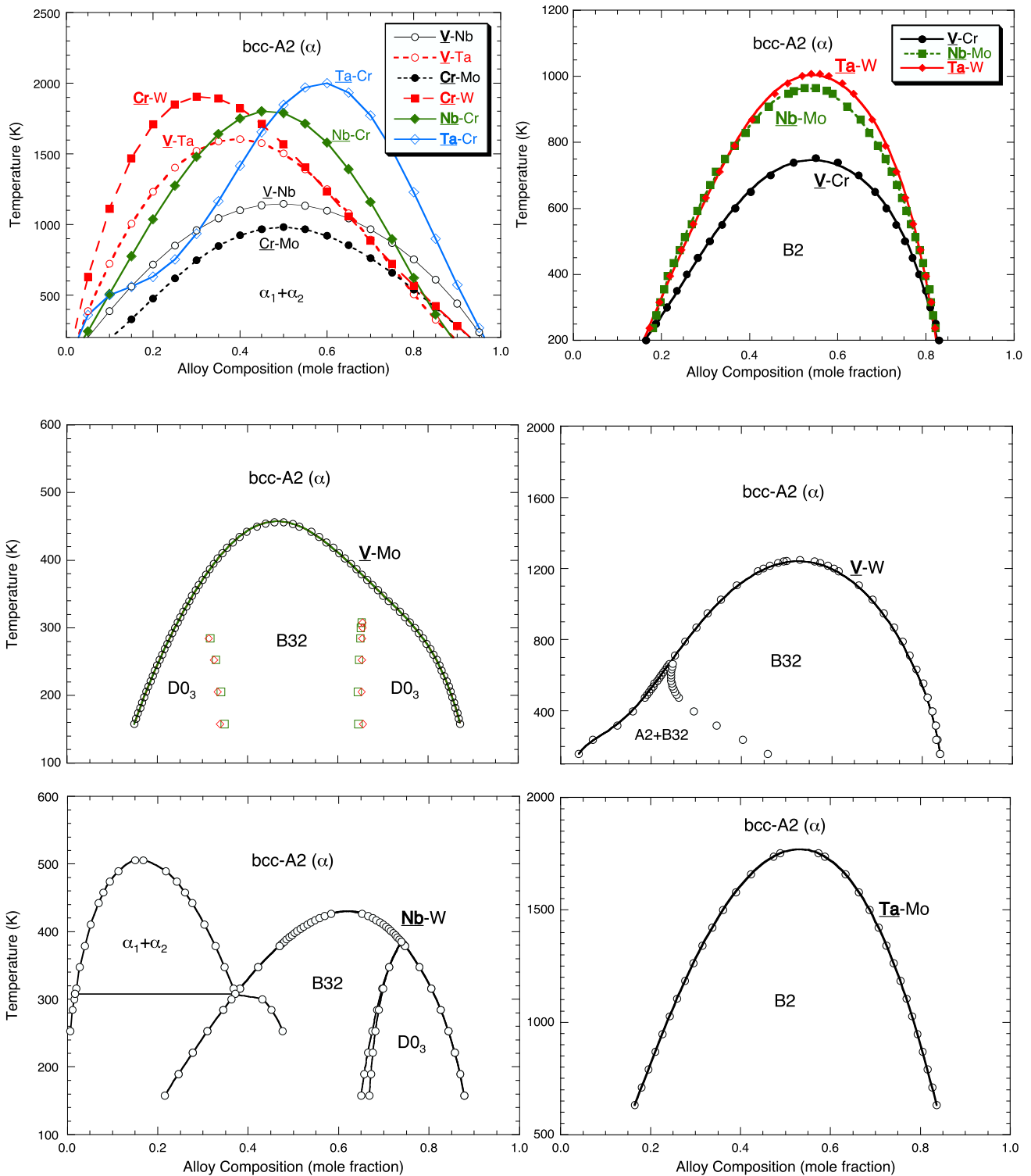


**Fig. 10** Predicted bcc-based alloy phase diagrams, as obtained from the tetrahedron approximation of the CVM with input from ab initio energetics. For all alloys the composition along the horizontal axis

refers to the second element of each alloy. (For interpretation of the references to color in this figure legend, the reader is referred to the web version of this article)

magnitude smaller than the contribution from the configurational configuration and ordering contributions. Hence, at least for this class of alloys, the vibrational free energy

has little effect on the predicted phase diagram displayed in Fig. 10.

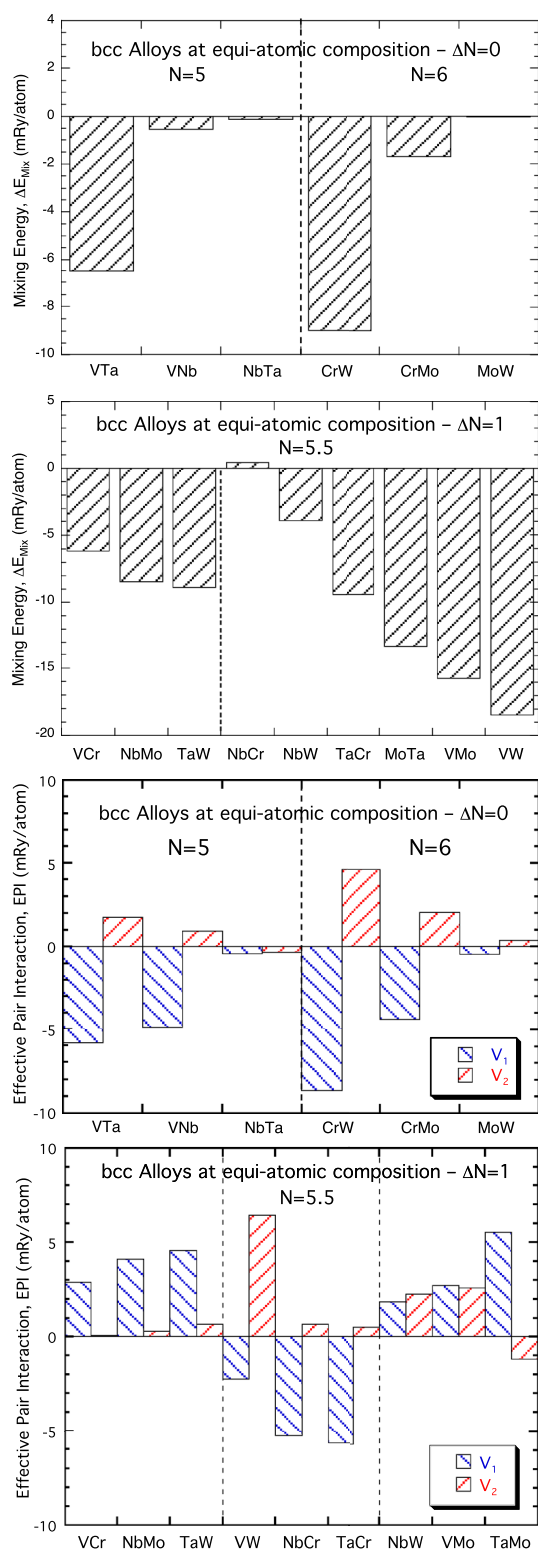


**Fig. 11** Mixing energy (top two figures) and first and second nearest neighbor effective pair interactions,  $V_1$  and  $V_2$  (bottom two figures), in mRy/atom, for bcc-based alloys at equi-atomic composition characterized by  $\Delta N = 0$  and  $\Delta N = 1$ , as obtained from TB-LMTO-CPA-GPM. (For interpretation of the references to color in this figure legend, the reader is referred to the web version of this article)

It is worth noting that since the order–disorder transition is second order in accordance with the results of the Landau theory of phase transitions, one would expect the SRO to exist well above the transition temperature, and also in a broad range of alloy composition, as it has been shown in the case of the Ta-W alloy system.<sup>[26]</sup> This property could help to identify, if not LRO, at least qualitatively, SRO that should be revealed on samples well annealed at relatively high temperature above the order–disorder transition temperature to promote the thermally activated ordering process; and performed by transmission electron microscopy (which is easy in the case of B2 since additional diffuse scattering intensities at the (100) and (300) reciprocal lattice positions should exist), and more quantitatively by anomalous x-ray diffuse scattering experiments at a synchrotron source or with neutron diffraction experiments. The confirmation of LRO may be more challenging because of an expected slow transformation kinetics at relatively low temperature.

Still on the experimental side, the existence of chemical order in alloys should obviously translates in a negative departure of the species-resolved activities<sup>[53]</sup> from linearity, as derived from electromotive force experiments, as a function of alloy composition (Raoult’s law). Qualitative experimental confirmation of chemical order in Nb-Mo,<sup>[9-11]</sup> Ta-W,<sup>[3-11]</sup> and Ta-Mo<sup>[10-11]</sup> is worth noting, with a large deviation of the activities from ideal behavior.

Finally, without drawing strong conclusions, the cleavage behavior is found for alloys that display order (e.g., Ta-Mo, Ta-W) whereas for those with very small tendency toward order or near ideality (such as Mo-W), a flow behavior is observed.<sup>[55]</sup> This change in mechanical response is consistent with the difference in the ordering trends that are predicted here.

## 5 Conclusion

Detailed calculations on electronic structure and related thermodynamic properties of the fifteen bcc-based TM alloys were carried out with the TB-LMTO formulation of the coherent potential approximation. The CPA and the GPM were used to obtain ordering tendencies and related thermodynamic information across the concentration range of these alloys. Temperature effects were accounted for within the generalized mean-field approach on which the CVM is based. The results from this work is summarized in Table 4, and among the fifteen alloys systems five (e.g., Cr-Mo, Cr-W) were already, at least qualitatively for some (i.e., Nb-Mo, Ta-Mo, Ta-W), confirmed.

Although the solid phase part of the phase diagrams (i.e., below the solidus line) reported in the literature is in most cases predicted, the second-order nature of the order–



**Table 4** Summary of the results of ground-state analysis of the Ising model for the 15 bcc-based alloys at equi-atomic composition

| Chemical tendency       | Alloy  |
|-------------------------|--|
| Phase separation        | V-Nb, V-Ta, Nb-Cr, Ta-Cr, <b>Cr-Mo, Cr-W</b> |
| Close to ideal solution | Nb-Ta, Mo-W                                  |
| B2 order                | V-Cr, Nb-Mo, Ta-Mo, Ta-W                     |
| B32 order               | V-Mo, V-W, Nb-W                              |

In bold are the alloys that have been confirmed experimentally

disorder transition can be used advantageously to identify short-range ordering at temperatures well above the order–disorder transition temperature. Anomalous dispersion x-ray diffuse scattering measurements at a synchrotron source<sup>[20]</sup> or neutron diffraction experiments should reveal unambiguously the nature of the SRO on samples well annealed at relatively high temperature to promote the thermally activated ordering process, and provide a quantitative measure of the EPIs that have been predicted in this study.

In the case of the bcc-based TM alloys, ordering (or clustering) trends can be rationalized in terms of the number of valence electron  $N$  (5 or 6) and the difference in the numbers of valence electrons  $\Delta N$  (0 or 1):  $\Delta N$  controls the tendency towards order or phase separation, and  $N$  controls its magnitude with an increase in the trend with  $N$  (Figs. 9, 11).

This study also shows the limitation of a phenomenological approach to thermodynamics since CALPHAD<sup>[56,57]</sup> cannot predict phases that are not experimentally confirmed, except in the cases of Cr-Mo and Cr-W that were finally known experimentally to exhibit phase separation.<sup>[1]</sup> For example, CALPHAD thermodynamic assessments have been proposed in the case of V-Mo,<sup>[12]</sup> and V-Ta,<sup>[58]</sup> by assuming the existence of bcc solid solution instead of B32 ordering and phase separation, respectively. It is also worth noting that, from our study, some of the phase diagrams display an asymmetry in composition, such as in the case of the three phase separating systems: V-Ta, Ta-Cr and Cr-W, and the alloys that display ordering: V-Cr, V-Mo, V-W, Nb-Mo, Nb-W, Ta-Mo, and Ta-W. That is a good example of what ab initio studies can provide to the CALPHAD methodology to enhance its power,<sup>[58]</sup> as was shown in the case of the Mo-Ta-W system,<sup>[27]</sup> although it is always wise to quantitatively confirm the predicted results from experiments. As a final remark, since the approach that was used here decouples the energetics of the reference chemically random state and the effective interactions that build up the ordering part of the energy, richer conclusions can be reached on alloy stability. For the present class of alloys,

the mixing energy in all cases is practically negative, i.e., favors alloy formation, whereas the interactions depending on the number of valence electrons and their difference controls the ordering trend. This differentiation among these two contributions also provided a theoretical explanation for transient ordering in alloys,<sup>[59]</sup> by recognizing that the kinetic behavior for phase separation is much slower than for ordering, but once again, experimental support is still required to fully confirmed this prediction.

**Acknowledgments** The original work from P. T. and contribution from A. P. were performed under the auspices of the U.S. Department of Energy by Lawrence Livermore National Laboratory under Contract DE-AC52-07NA27344. Work at LLNL by A. P. was funded by the Laboratory Directed Research and Development Program under project tracking code 21-ERD-037. The work of V. D. and J. K. was supported by the Czech Science Foundation (Project No. 18-07172S).

## References

1. T. Massalski and P.R. Subramanian, *Binary Alloy Phase Diagrams*, ASM international, Cleveland, 1990
2. R. Krishnan, S.P. Garg, and N. Krishnamurthy, Tantalum–Tungsten System, *J. Alloys Phase Diag.*, 1987, **3**(1), p 1-3
3. S.C. Singhal and W.L. Worrell, High-Temperature Thermodynamic Properties of Solid Ta-W Alloys, *Met. Trans.*, 1973, **4**, p 895-898. <https://doi.org/10.1007/BF02645586>
4. H.J. Goldschmidt and J.A. Brand, The Constitution of the Chromium-Niobium-Molybdenum System, *J. Less-Common Met.*, 1961, **3**, p 44-61. [https://doi.org/10.1016/0022-5088\(61\)90042-X](https://doi.org/10.1016/0022-5088(61)90042-X)
5. C. Schmetterer, A. Khvan, A. Jacob, B. Hallstedt, and T. Markus, A New Theoretical Study of the Cr-Nb System, *J. Phase Equilib. Diffus.*, 2014, **35**, p 434-444. <https://doi.org/10.1007/s11669-014-0313-y>
6. H.J. Goldschmidt and J.A. Brand, The Constitution of the Chromium-Niobium-Silicon System, *J. Less-Common Met.*, 1961, **3**, p 34-43. [https://doi.org/10.1016/0022-5088\(61\)90041-8](https://doi.org/10.1016/0022-5088(61)90041-8)
7. H. Okamoto, Cr-Ta (Chromium-Tantalum), *J. Phase Equilib. Diffus.*, 2006, **27**, p 199. <https://doi.org/10.1007/s11669-006-0060-9>
8. G. Ghosh, Thermodynamic and Kinetic Modeling of the Cr-Ti-V System, *J. Phase Equilib.*, 2002, **23**(4), p 310-328. <https://doi.org/10.1361/105497102770331569>
9. S.C. Singhal and W.L. Worrell, A High-Temperature Thermodynamic Investigation of the Nb-Mo System, *Met. Trans.*, 1973, **4**, p 1125-1128. <https://doi.org/10.1007/BF02645616>
10. R. Predmore and R.J. Arsenault, Short-Range Order of Ta-Mo Bcc Alloys, *Scr. Metall.*, 1970, **4**, p 213-218. [https://doi.org/10.1016/0036-9748\(70\)90195-X](https://doi.org/10.1016/0036-9748(70)90195-X)
11. S.C. Singhal and W.L. Worrell, An EMF study of the high-temperature thermodynamic properties of solid tantalum-molybdenum alloys, in *Metallurgical Chemistry—Proceedings of a symposium held at Brunel University and the National Physical Laboratory*, 1972, 1.5–1, 65
12. J. Bratberg and K. Frisk, A Thermodynamic Analysis of the Mo-V and Mo-V-C Systems, *Calphad*, 2002, **26**(3), p 459-476. [https://doi.org/10.1016/S0364-5916\(02\)00057-3](https://doi.org/10.1016/S0364-5916(02)00057-3)
13. R.T. Begley and J.H. Bechtold, Effect of Alloying on the Mechanical Properties of Niobium, *J. Less-Common Met.*, 1961, **3**, p 1-12. [https://doi.org/10.1016/0022-5088\(61\)90037-6](https://doi.org/10.1016/0022-5088(61)90037-6)

14. J.F. Smith and O.N. Carlson, The Ta-V (Tantalum-Vanadium) System, *J. Phase Equilib.*, 1983, **4**(3), p 284-289. <https://doi.org/10.1007/BF02868668>
15. J.F. Smith and O.N. Carlson, Ta-V (Tantalum-Vanadium), *Phase Diagrams of Binary Vanadium Alloys*, ASM International, Cleveland, 1989, p 276-282
16. C.A. Danon and C. Servant, A Thermodynamic Evaluation of the Ta-V System, *J. Alloys Compd.*, 2004, **366**, p 191-200. [https://doi.org/10.1016/S0925-8388\(03\)00728-X](https://doi.org/10.1016/S0925-8388(03)00728-X)
17. H. Okamoto, Ta-V (Tantalum-Vanadium), *J. Phase Equilib. Diffus.*, 2005, **26**, p 298-299. <https://doi.org/10.1007/s11669-005-0127-z>
18. J. Hohe and P. Gumbsch, On the Potential of Tungsten-Vanadium Composites for High Temperature Application with Wide-Range Thermal Operation Window, *J. Nucl. Mater.*, 2010, **400**, p 218-231. <https://doi.org/10.1016/j.jnucmat.2010.03.007>
19. R.W. Cahn, The Place of Atomic Order in the Physics of Solids in Metallurgy, *Springer Series in Materials Science*, Vol 27, F.E. Fujita, Ed., Springer, Berlin, 1994
20. O.N. Senkov, G.B. Wilks, D.B. Miracle, C.P. Chuang, and P.K. Liaw, Refractory High-Entropy Alloys, *Intermetallics*, 2010, **18**, p 1758-1765. <https://doi.org/10.1016/j.intermet.2010.05.014>
21. F. Ducastelle and F. Gautier, Generalized Perturbation Theory in Disordered Transitional Alloys: Applications to the Calculation of Ordering Energies, *J. Phys. F: Met. Phys.*, 1976, **6**(11), p 2039-2062. <https://doi.org/10.1088/0305-4608/6/11/005>
22. F. Ducastelle, Order and Phase Stability in Alloys, *Cohesion and Structure Series*, Vol 3, F.R. de Boer and D.G. Pettifor, Ed., North-Holland, Amsterdam, 1991
23. J.S. Faulkner, The Modern Theory of Alloys, *Prog. Mater. Sci.*, 1982, **27**(1-2), p 1-187. [https://doi.org/10.1016/0079-6425\(82\)90005-6](https://doi.org/10.1016/0079-6425(82)90005-6)
24. I. Turek, V. Drchal, J. Kudrnovsky, M. Sob, and P. Weinberger, *Electronic Structure of Disordered Alloys, Surfaces and Interfaces*, Kluwer Academic Publishers, Boston-London-Dordrecht, 1997
25. R. Kikuchi, A Theory of Cooperative Phenomena, *Phys. Rev.*, 1981, **81**, p 988-1002. <https://doi.org/10.1103/PhysRev.81.988>
26. P.E.A. Turchi, A. Gonis, V. Drchal, and J. Kudrnovsky, First-principles study of stability and local order in substitutional Ta-W alloys, *Phys. Rev. B*, 2001, **64**, p 085112-1-085112-8. <https://doi.org/10.1103/PhysRevB.64.085112>
27. P.E.A. Turchi, V. Drchal, J. Kudrnovsky, C. Colinet, L. Kaufman, and Z.-K. Liu, Application of ab initio and CALPHAD thermodynamics to Mo-Ta-W alloys, *Phys. Rev. B*, 2005, **71**, p 094206-1-094206-14. <https://doi.org/10.1103/PhysRevB.71.094206>
28. P.E.A. Turchi, Electronic Theories of Alloy Phase Stability, *Intermetallic Compounds: Principles and Practice*, Vol 1, J.H. Westbrook and R.L. Fleischer, Ed., Wiley, New York, 1995, p 21-54
29. D.M. Ceperley and B.J. Alder, Ground State of the Electron Gas by a Stochastic Method, *Phys. Rev. Lett.*, 1980, **45**, p 566-568. <https://doi.org/10.1103/PhysRevLett.45.566>
30. J.P. Perdew and A. Zunger, Self-Interaction Correction to Density-Functional Approximations for Many-Electron Systems, *Phys. Rev. B*, 1981, **23**(10), p 5048-5079. <https://doi.org/10.1103/PhysRevB.23.5048>
31. S.H. Wei, L.G. Ferreira, J.E. Bernard, and A. Zunger, Electronic Properties of Random Alloys: Special Quasirandom Structures, *Phys. Rev. B*, 1990, **42**, p 9622-9649. <https://doi.org/10.1103/PhysRevB.42.9622>
32. C. Jiang, C. Wolverton, J. Sofo, L.-Q. Chen, and Z.-K. Liu, First-Principles Study of Binary Bcc Alloys Using Special Quasi-Random Structures, *Phys. Rev. B*, 2004, **69**(21), p 214202-1-214202-10. <https://doi.org/10.1103/PhysRevB.69.214202>
33. M. Muzyk, D. Nguyen-Manh, J. Wrobel, K.J. Kurzydowski, N.L. Baluc, and S.L. Dudarev, First-Principles Model for Phase Stability, Radiation Defects and Elastic Properties of W-Ta and W-V Alloys, *J. Nucl. Mater.*, 2013, **442**, p S680-S683. <https://doi.org/10.1016/j.jnucmat.2012.10.025>
34. A. Gonis, Green Functions for Ordered and Disordered Systems, *Studies in Mathematical Physics*, Vol 4, E. van Groesen and E.M. de Jager, Ed., North Holland, Amsterdam, 1992
35. C. Colinet, A. Bessoud, and A. Pasturel, Theoretical determinations of thermodynamic data and phase diagrams of bcc binary transition-metal alloys, *J. Phys. F: Met. Phys.*, 1988, **18**, p 903-921. <https://doi.org/10.1088/0305-4608/18/5/010>
36. R.J. Hawkins, M.O. Robbins, and J.M. Sanchez, Electronic-structure calculations of binary alloy phase diagrams, *Phys. Rev. B*, 1986, **33**(7), p 4782-4792
37. G. Kresse and J. Furthmuller, Efficiency of Ab-Initio Total Energy Calculations for Metals and Semiconductors Using a Plane-Wave Basis Set, *Comput. Mater. Sci.*, 1996, **6**(1), p 15-50. [https://doi.org/10.1016/0927-0256\(96\)00008-0](https://doi.org/10.1016/0927-0256(96)00008-0)
38. G. Kresse and J. Furthmuller, Efficient Iterative Schemes for Ab Initio Total-Energy Calculations Using Plane-Wave Basis Set, *Phys. Rev. B*, 1996, **54**(16), p 11169-11186. <https://doi.org/10.1103/PhysRevB.54.11169>
39. G. Kresse and D. Joubert, From Ultrasoft Pseudopotentials to the Projector Augmented-Wave Method, *Phys. Rev. B*, 1999, **59**(3), p 1758-1775. <https://doi.org/10.1103/PhysRevB.59.1758>
40. C. Jiang, First-Principles Study of Ternary Bcc Alloys Using Special Quasi-Random Structures, *Acta Mater.*, 2009, **57**, p 4716-4726. <https://doi.org/10.1016/j.actamat.2009.06.026>
41. V. Blum and A. Zunger, Prediction of Ordered Structures in the Bcc Binary Systems of Mo, Nb, Ta, and W from First-Principles Search of Approximately 3,000,000 Possible Configurations, *Phys. Rev. B*, 2005. <https://doi.org/10.1103/PhysRevB.72.020104>
42. J.W.D. Connolly and A.R. Williams, Density-Functional Theory Applied to Phase Transformations in Transition-Metal Alloys, *Phys. Rev. B*, 1983, **27**(8), p 5169-5172
43. P.E.A. Turchi, V. Drchal, and J. Kudrnovsky, Stability and Ordering Properties of fcc-Based Alloys Based on Rh, Ir, Pd, and Pt, *Phys. Rev. B*, 2006, **74**, p 064202-1-064202-12. <https://doi.org/10.1103/PhysRevB.74.064202>
44. M. Hennion, Chemical SRO Effects in Ferromagnetic Fe Alloys in Relation to Electronic Band Structure, *J. Phys. F: Met. Phys.*, 1983, **13**(11), p 2351-2358. <https://doi.org/10.1088/0305-4608/13/11/017>
45. A. Gonis, P.P. Singh, P.E.A. Turchi, and X.G. Zhang, Use of the Ising Model in the Study of Substitutional Alloys, *Phys. Rev. B*, 1995, **51**(4), p 2122-2131. <https://doi.org/10.1103/PhysRevB.51.2122>
46. J.M. Sanchez, F. Ducastelle, and D. Gratias, Generalized Cluster Description of Multicomponent Systems, *Phys. A*, 1984, **128**(1-2), p 334-350. [https://doi.org/10.1016/0378-4371\(84\)90096-7](https://doi.org/10.1016/0378-4371(84)90096-7)
47. J.M. Sanchez, Cluster Expansions and the Configurational Energy of Alloys, *Phys. Rev. B*, 1993, **48**(18), p 14013-14015
48. J.M. Sanchez, Cluster Expansion and the Configurational Theory of Alloys, *Phys. Rev. B*, 2010, **81**(22), p 224202-1-224202-13. <https://doi.org/10.1103/PhysRevB.81.224202>
49. J.M. Sanchez, Renormalized Interact Ions in Truncated Cluster Expansions, *Phys. Rev. B*, 2019, **99**(13), p 134206-1-134206-18. <https://doi.org/10.1103/PhysRevB.99.134206>
50. Finel, Thèse de Doctorat d'Etat es Sciences Physiques, University Paris VI, France, unpublished (1987); and Technical Report (ONERA 1987-3 (unpublished))
51. A. Finel and F. Ducastelle, *Phase Transformations in Solids*, T. Tsakalakos, Ed., North-Holland, Amsterdam, 1984, p 293
52. A. Finel, D. Gratias, and R. Portier, *L'Ordre et le Désordre dans les Matériaux*, Les Editions de Physique, Les Ulis, 1984, p 9

53. N.S. Golosov and A.M. Tolstik, Theory of Order–Disorder and Order–Order Transformations in Binary Alloys with Bcc Lattice—I: Free Energy and Phase Equilibrium Equations, *J. Phys. Chem. Solids*, 1975, **36**(9), p 899-902. [https://doi.org/10.1016/0022-3697\(75\)90165-1](https://doi.org/10.1016/0022-3697(75)90165-1)
54. C. Bichara and G. Inden, A combined Monte Carlo and cluster variation approach for calculating Gibbs energies and chemical potentials, in *Statics and Dynamics of Alloy Phase Transformations*, edited by P.E.A. Turchi and A. Gonis, NATO Advanced Studies Institute, Series B: Physics, Vol 319, Plenum Press, New York, 1994, p 541
55. L.I. van Torne and G. Thomas, Structure and Mechanical Properties of Ta-Mo Alloy Single Crystals, *Acta Metall.*, 1966, **14**(5), p 621-635. [https://doi.org/10.1016/0001-6160\(66\)90070-8](https://doi.org/10.1016/0001-6160(66)90070-8)
56. L. Kaufman and H. Bernstein, *Computer Calculation of Phase Diagrams with Special Reference to Refractory Metals, Refractory Materials*, Academic Press, London, 1970
57. B. Sundman, B. Jansson, and J.-O. Andersson, The Thermo-Calc Databank System, *Calphad*, 1985, **9**(2), p 153-190. [https://doi.org/10.1016/0364-5916\(85\)90021-5](https://doi.org/10.1016/0364-5916(85)90021-5)
58. P.E.A. Turchi, I.A. Abrikosov, B. Burton, S.G. Fries, G. Grimvall, L. Kaufman, P. Korzhavyi, V. Rao Manga, M. Ohno, A. Pisch, A. Scott, and W. Zhang, Interface Between Quantum-Mechanical-Based Approaches, Experiments, and CALPHAD Methodology, *Calphad*, 2007, **31**, p 4-27. <https://doi.org/10.1016/j.calphad.2006.02.009>
59. L. Reinhard and P.E.A. Turchi, Transient Ordered States in Phase-Separating Alloys, *Phys. Rev. Lett.*, 1994, **72**(1), p 120-123. <https://doi.org/10.1103/PhysRevLett.72.120>

**Publisher's Note** Springer Nature remains neutral with regard to jurisdictional claims in published maps and institutional affiliations.